

Observation of Enhanced Core Impurity Transport in a Turbulence-Reduced Stellarator Plasma

Daniel Medina-Roque,^{1,*} Isabel García-Cortés,¹ Naoki Tamura,² Kieran J. McCarthy,¹ Federico Nespoli,³ Kenji Tanaka,^{4,6} Mamoru Shoji,^{4,5} Suguru Masuzaki,^{4,5} Hisamichi Funaba,⁴ Chihiro Suzuki,^{4,5} Albert Mollen,³ Robert Lunsford,³ Katsumi Ida,⁴ Mikiro Yoshinuma,⁴ Motoshi Goto,^{4,5} Yasuko Kawamoto,^{4,5} Tomoko Kawate,⁷ Tokihiko Tokuzawa,^{4,5} Ichihiko Yamada^{4,5}

¹Laboratorio Nacional de Fusión, CIEMAT, Madrid, Spain

²Max-Planck Institute for Plasma Physics, Greifswald, Germany

³Princeton Plasma Physics Laboratory, Princeton, NJ, USA

⁴National Institute for Fusion Science, National Institutes of Natural Science, Toki, Japan

⁵The Graduate University of Advanced Studies, SOKENDAI, Toki, Japan

⁶Interdisciplinary Graduate School of Engineering Sciences, Kyushu University, Kasuga, Japan

⁷National Institutes for Quantum Science and Technology, Naka Institute for Fusion Science and Technology, Naka, Japan

ABSTRACT. An enhancement of core impurity transport is observed for the first time in a high-density stellarator plasma with continuous lithium (Li) granule injection. When Li-granules are dropped continuously into the plasma, energy confinement is improved due to reduced turbulence. In parallel, the transport of mid- and high-Z impurities is increased. Simulations with the drift-kinetic transport code SFINCS for such plasmas show that the role of neoclassical transport prevails for the main plasma components (electrons, ions, and $Z_{\text{avg}} = 3.5$). In contrast, the classical contribution is dominant in transporting high-Z impurities. This study demonstrates experimentally, for the first time also, that classical transport plays an essential role in enhancing the transport of such impurities in high-density stellarator plasmas, a situation that is achieved by continuous injection of Li-granules, which is effective for real-time wall conditioning and plasma performance improvement.

A crucial challenge for developing stellarator-type devices as fusion reactors is the identification of operational scenarios that ensure long bulk ion particle and energy confinement and impurity accumulation avoidance, especially for high-Z elements that can induce plasma radiative collapse [1]. This is most challenging for high-density regimes in which confinement is extended due to the creation of an inwards-directed ambipolar radial electric field (ion-root) and a drop in diffusive impurity transport [2, 3]. Indeed, the reduction of anomalous transport due to plasma turbulence is a standard means to improve fuel particle confinement [4]. However, this can also enhance impurity confinement and lead to accumulation, as observed experimentally and predicted by neoclassical (NC) simulations [1]. In the Large Helical Device (LHD), an impurity hole (extremely hollow profile of impurities) has been observed in low-density and high-ion-temperature plasmas, and the neoclassical/anomalous transport of such plasmas is studied extensively [5-8]. While Ion Temperature Gradient (ITG) turbulence induces inward-directed impurity fluxes [7, 8], detailed NC simulations revealed that thermo-diffusion plays an essential role in outward impurity fluxes. On the other hand, in high-density LHD plasmas, additional electron cyclotron resonance heating (ECRH) is found to pump out the impurities from the core region only [9, 10], albeit the physical mechanisms remain unclear.

Here, we perform TESPEL (Tracer-Encapsulated Solid Pellet) injections [11] during continuous lithium (Li-) granule dropping into high-density, low-ion-temperature plasmas of LHD to study the core impurity transport in such plasmas. It is found that Li-granule dropping induces an improvement of confinement similar to that observed during low-Z (B, BN, or C) powders dropping [12, 13, 14]. Contrary to expectations, however, clear reductions in

confinement time of impurities injected by TESPEL are observed when Li-granules are dropped into the plasmas. In this letter, we provide the first experimental evidence that continuous Li-granule dropping reduces the confinement time of mid/high-Z impurities in high-density stellarator plasmas, where the negative radial electric field could exist across the full plasma radius. The simulation results indicate that the classical contribution significantly enhances impurity transport in the core plasma.

As noted above, the experiments shown here are performed in the LHD, the largest superconducting heliotron-type device with a major radius of 3.9 m, a minor radius of 0.6 m and typical plasma volume of 30 m³ [15]. A comprehensive collection of diagnostics is available [16]. Those of interest include Charge-Exchange recombination Spectroscopy (CXs) [17], 2-dimensional Phase Contrast Imaging (2D-PCI) [18], visible Bremsstrahlung measurement [19], as well as Vacuum and Extreme Ultraviolet (VUV/EUV) spectrometers [20]. LHD is equipped with an Impurity Powder Dropper, which allows the injection of sub-millimeter impurity grains by gravity [21]. The TESPEL, which allow us to inject known quantities of impurities at pre-determined radii and times [22, 23], is used for titanium (Ti) and molybdenum (Mo) impurity injection. Experiments are conducted with the so-called inward-shifted magnetic configuration, vacuum magnetic axis position at $R_{\text{ax}} = 3.6$ m and magnetic field strength at the magnetic axis of $B_{\text{ax}} = 2.75$ T. Hydrogen (H₂) gas is used as a working gas. The heating pattern applied is 3 MW of ECRH power from 3 s to 5 s together with 3 MW of tangential NBI from 3.3 s to 5 s, with tangential NBI heating being increased to 7 MW from 5 s to 7 s and 4 MW of perpendicular modulated NBI for the CXs diagnostic. The typical plasma parameters are line-averaged density $n_{e,\text{avg}} \sim 5.3 \times 10^{19}$ m⁻³, central electron temperature $T_{e,0} \sim 2.4$ keV and diamagnetic energy $W_p \sim 880$ kJ. Li-granules are dropped continuously into the plasmas from ~ 4.8 s until discharge end (this is

*Contact author: daniel.medina@ciemat.es

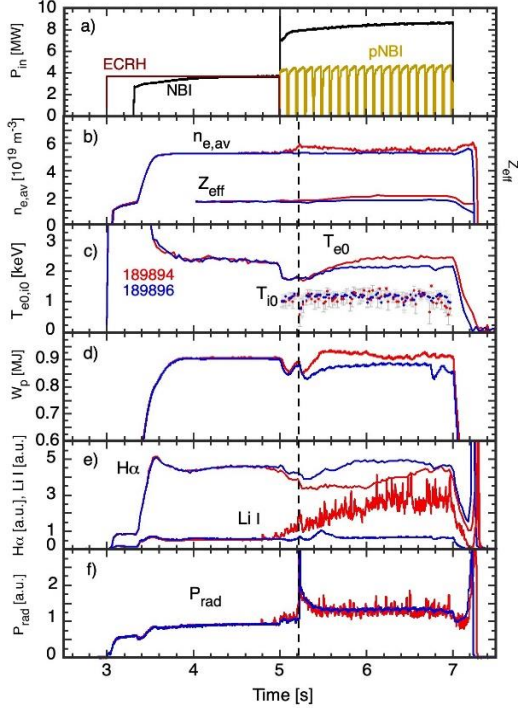


Figure 1. Time traces of a) ECRH, tangential (NBI) and perpendicular (pNBI) neutral beams, b) line-averaged electron density, $n_{e,av}$, and Z_{eff} (from 4 s to 7.2 s for clarity), c) central T_e and T_i , d) stored plasma energy (short dip at $t \sim 6.8$ s correspond to brief NBI breakdown), e) Balmer $H\alpha$ (656.3 nm) and Li I (670.8 nm) emissions, and f) total radiated power, P_{rad} for #189894 (with Li-granules and Mo-TESPEL injection - red) and #189896 (reference shot without Li-granules but with Mo-TESPEL injection - blue). TESPEL injections are made at 5.225 s (vertical dash – dash).

identified by Li I emissions (see Fig.1 e)). Comparing signals for discharges with and without Li-granule dropping, it is found that Li-granule dropping modifies various parameters, *e.g.*, $n_{e,av}$ increases slightly with $\Delta n_{e,av}/n_{e,av} < 5\%$, T_{e0} rises where $\Delta T_{e0}/T_{e0} \sim 12.5\%$, plasma stored energy, W_p , grows by $\sim 10\%$ higher and Z_{eff} goes up from ~ 1.8 to ~ 2.3 . Moreover, the observed $\sim 25\%$ reduction in $H\alpha$ emission might indicate a reduction of particle fueling under almost constant line-averaged electron density. This would be compatible with an improvement in bulk-ion particle confinement. However, due to time varying gas fueling by feedback control, and possible changes in wall recycling due to Li granules, a complete particle balance analysis, like Ref. [24], would be needed to confirm this point.

It is seen also that Li-granules modify profile shapes. For instance, in Figure 2, n_e increases in the edge region ($0.7 < r_{eff}/a_{99} < 1$) while remaining constant in

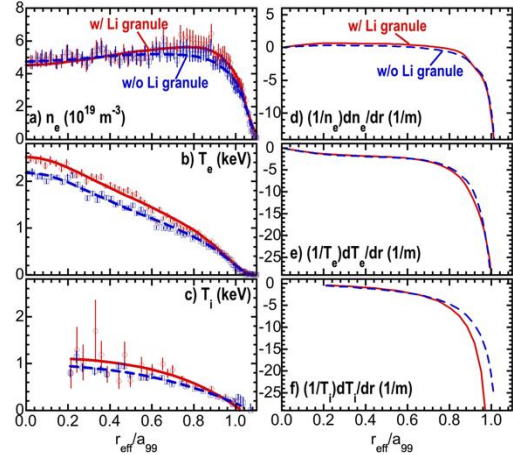


Figure 2. Radial profiles of a) electron density, b) electron temperature and c) ion temperature at $t \sim 6$ s for #189894 (with Li granules - red) and #189896 (without Li granules - blue). Also shown are inversed scale lengths of d) electron density, $L_{n_e}^{-1}$, e) electron temperature, $L_{T_e}^{-1}$, and f) ion temperature, $L_{T_i}^{-1}$, at $t \sim 6$ s. pNBI attenuation limits reliable T_i measurement to $r_{eff}/a_{99} > 0.2$. In both cases, a Mo-TESPEL is injected at $t = 5.225$ s.

the core ($r_{eff}/a_{99} < 0.7$). Here, r_{eff} and a_{99} denote effective minor radius and minor radius, respectively, within which 99 % of total plasma stored energy is confined. This rise in edge density leads to a slightly hollower density profile. Moreover, both core T_e and T_i are seen to increase during Li-granule dropping, the latter despite the large error bars. Finally, whilst the inversed scale lengths of n_e and T_e appear to be almost identical for both situations, the inversed scale length of T_i seems to increase during Li-granule dropping at $r_{eff}/a_{99} > 0.8$.

In order to evaluate impurity confinement times with/without Li-granules, an impurity is injected with TESPEL at 5.225 s, as indicated by a dashed vertical line in Figure 1. Ti ($Z = 22$) and Mo ($Z = 42$) impurities are injected to identify possible Z dependence of impurity transport. The amounts of impurity particles are as follows: 2.94×10^{17} Ti atoms for #189891, 2.82×10^{17} Ti atoms for #189893, 4.98×10^{17} Mo atoms for #189894, and 5.92×10^{17} Mo atoms for #189896. The deposition locations of impurities injected with TESPEL are estimated around $r_{eff}/a_{99} = 0.75$, which is inside the density profile shoulder. A TESPEL injection causes a small transient rise in $n_{e,av}$, a 5% decrease in plasma stored energy that recovers fully after 200 ms, and a 50% reduction in T_i that recovers its pre-injection level after ~ 50 ms. Figure 3 shows the temporal evolutions of Ti XX (25.93 nm) and Mo XXX II (12.79 nm) measured with the EUV/VUV spectrometer, SOXMOS [25]. The data points shown

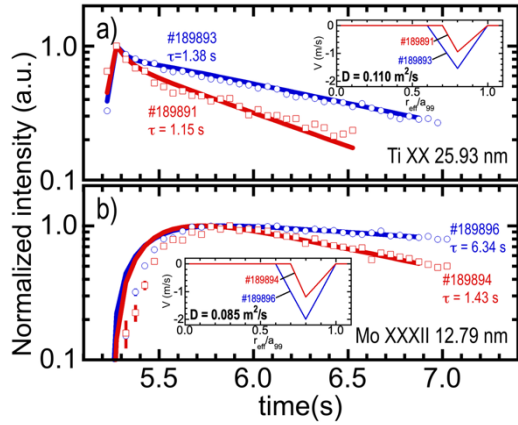


Figure 3. Semi-log plots of normalized intensities of a) Ti XX and b) Mo XXXII: evaluated (open squares) and STRAHL code predictions (solid lines) for #189893 and #189896 (without Li-granules - blue) and for #189891 and #189894 (with Li-granules - red). TESPELS are injected at 5.225 s. Inserted plots show convective velocity profiles and diffusion coefficients used for STRAHL. Impurity confinement times (decay times), τ , are obtained by fits to experimental data. The error bars for the data points evaluated are included.

in Fig. 3 are obtained by integrating under their emission line curves while considering the continuum level. The Ti confinement time without Li granules is estimated as 1.38 s, and that with Li granules is estimated as 1.15 s (~ 17 % reduction). Next, the Mo confinement time without Li granules is estimated as 6.34 s, and that with Li granules is estimated as 1.43 s (~ 78 % reduction). Therefore, it appears that the higher the Z impurity, the more the impurity confinement time is reduced in plasma with Li granules. For these plasmas, we performed simulations using the STRAHL impurity transport code [26, 27] with radially flat diffusion coefficients, D. Solid lines in Fig.3 show the STRAHL results. The temporal evolution of Ti XX without Li granules is well reproduced with $D = 0.11 \text{ m}^2/\text{s}$ and the convection velocity, V, profile (minimum V of -1.55 m/s) shown by the sub-plot in Fig. 3a). For the temporal evolution of Ti XX with Li granules, the same D and a slightly narrower negative V profile (minimum V of -0.95 m/s) can reproduce the experimental results. We find that if the root-square dependence of charge is applied, the temporal evolutions of Mo XXXII are also well reproduced, *i.e.*, $0.11 \text{ m}^2/\text{s} \times \sqrt{Z_{\text{Ti}^{19+}}/Z_{\text{Mo}^{31+}}} \sim 0.085 \text{ m}^2/\text{s}$, $-1.55 \text{ m/s} \times \sqrt{Z_{\text{Mo}^{31+}}/Z_{\text{Ti}^{19+}}} \sim -2.0 \text{ m/s}$ (without Li), $-0.95 \text{ m/s} \times \sqrt{Z_{\text{Mo}^{31+}}/Z_{\text{Ti}^{19+}}} \sim -1.2 \text{ m/s}$ (with Li). There is no simple dependence of charge itself on the results obtained by STRAHL, which might indicate that a mixture of collisional and turbulent components affects the impurity transport observed. Indeed, the D suggested by SFINCS is 4 ~ 5

times smaller than that indicated by STRAHL. Although the V calculated by SFINCS has a different sign from the V produced by STRAHL, it is found to become more positive during Li-injection for both. Thus lower inward pinch for plasmas with Li granules is foreseen by both codes. Moreover, the STRAHL results suggest that the impact region of Li granule dropping on core impurity transport is the same for both Ti and Mo impurities. Discrepancies between experimental observations and STRAHL calculations exist in the initial phase of Mo XXXII evolutions. Introducing the spatially varied diffusion coefficient might eliminate these. However, since the latter phase, where the impurity confinement degradation (difference with and without Li) is prominent, of the temporal evolution of impurity line emissions is currently well-reproduced by STRAHL results, further complete matching between experiment and simulations will be left for another occasion.

It is crucial to understand how Li-granule dropping modifies the impurity transport in the range of $r_{\text{eff}}/a_{99} > 0.6$. First, it is unlikely that impurity transport will increase due to reduced turbulence. Next, we consider the radial electric field, E_r , a crucial factor in impurity transport in high-density LHD plasmas. Here, the CXS diagnostic can estimate E_r only in the region of $r_{\text{eff}}/a_{99} > 0.8$ due to high plasma density, which results in strong attenuation of the probe neutral beam. The E_r estimated by CXS shows similar negative values regardless of the presence or absence of Li granules. No changes in E_r have been confirmed in other ways also. Next, the 2D-PCI diagnostic measures ion scale turbulence, where $k = 0.1 - 0.8 \text{ mm}^{-1}$, $f = 20 - 500 \text{ kHz}$. As shown in Fig. 4 a), the fluctuation amplitudes measured with the 2D-PCI are reduced significantly in #189894. Here, the dominant turbulence is more likely to be Resistive Interchange (RI) turbulence [28], since the ITG is presumably stable, *i.e.*, the threshold for ITG is $L_{\text{Ti}}^{-1} \sim 2.5 \text{ m}^{-1}$ [29]. A reduction in RI turbulence provides a possible explanation for improved energy confinement. Figure 4 b) shows fluctuation phase

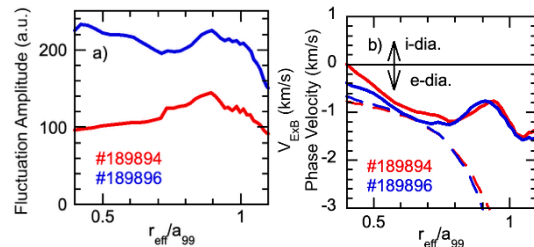


Figure 4. Radial profiles of a) fluctuation amplitude and b) fluctuation phase (solid) at 6 s estimated with 2D-PCI and V_{ExB} velocities estimated by SFINCS (dash - dash) for #189894 (with Li-granule dropping - red) and #189896 (reference, without Li-granules - blue).

velocities in the laboratory frame in which poloidal components dominate the measured k-components. Thus, the phase velocities are considered close to ExB poloidal rotation velocities. The E_r indicated by the phase velocities are negative and almost identical for with and without Li-granules. In Fig. 4 b), the V_{ExB} predicted by the collisional transport code SFINCS [30, 31] for both cases is also shown, and those are similar to the phase velocities measured with the 2D-PCI in the range of $0.4 < r_{\text{eff}}/a_{99} < 0.7$. Moreover, the V_{ExB} predicted by the SFINCS is also almost identical in the region shown with and without Li-granules.

Given the need to further understand underlying physics, classical and neo-classical particle fluxes predicted by the SFINCS for with and without Li-granule dropping are compared. As shown in Fig. 5, total electron and proton fluxes are dominated by the NC contribution and they increase in the case of Li-granule dropping (#189894). In the simulations, an ‘‘average’’ impurity ion with average charge equal to ~ 3.5 is considered to account for He, Li and C, and, for simplicity, the averaged impurity density profile is assumed to be the same as the electron density. This reduces the cost of simulations since the system being

solved grows with the number of species and the results are substantially the same in terms of E_r and bulk particle fluxes. It is found that NC fluxes, which dominate for the averaged impurity, become more negative at all radii with Li to maintain ambipolarity. Finally, total Mo^{+31} particle fluxes are generally outward-directed and dominated by the classical contribution at all radii for #189896 (without Li) and become significantly more positive outside $r_{\text{eff}}/a_{99} \sim 0.45$ in #189894 (with Li). It should be noted that coronal equilibrium is assumed for the Mo^{+31} ion density profile in the simulation, this being at trace level to avoid modifying Z_{avg} significantly. Similar results are obtained when a Gaussian density profile, centered around its expected deposition position, is assumed for Mo (more details about these SFINCS results and additional simulations including the variation of electrostatic potential on the flux surfaces will be presented in another paper). The experimental findings are aligned with previous simulation-based predictions for impurity transport [31], where classical transport is found to exceed the NC contribution for mid-Z species in the NC-optimized stellarator W7-X. Empirically, classical transport has been considered negligible relative to other transport channels (NC and turbulent). However, this study provides the first experimental evidence that classical transport can be crucial in transporting core impurities under specific plasma conditions, especially when Li-granules are dropped at the peripheral region.

In summary, continuous Li-granule dropping in the high-density LHD plasmas leads to improved energy confinement due to reduced turbulence and enhanced transport of mid-/high-Z impurities in the core plasmas. The STRAHL and SFINCS simulations indicate that the classical transport channel enhances core impurity transport in the $r_{\text{eff}}/a_{99} > 0.6$ region when Li-granules are dropped. To date, classical transport has been considered relevant for mid-Z impurities in the W7-X device [32] due to its NC optimized design. However, our results indicate that enhancement of impurity transport due to classical mechanisms can also occur in devices without NC optimization, such as LHD, under specific plasma conditions. Generally, the preferred condition is as low as possible NC transport channel (i.e., NC inward and outward fluxes being close to balanced). Such a condition might be achieved in tokamak plasmas also, such as in ITER, but this would require future simulations and experiments. This paper reports important findings for future fusion devices, where the primary concern is

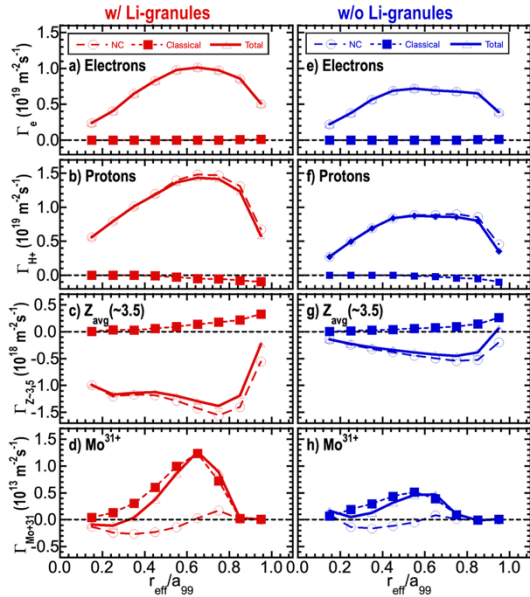


Figure 5. NC (open circles, long dash-dash), classical (squares, short dash-dash) and total (open triangles, continuous) particle fluxes normalized to pseudo-densities for a) electrons, b) H^+ ion, c) effective impurity contents with $Z_{\text{avg}} = \sim 3.5$ and d) trace Mo^{+31} ions as a function of normalized minor radius. Predictions are made with the SFINCS code for #189894 (left, with Li-granule dropping - red) and #189896 (right, without Li-granule dropping - blue).

impurity accumulation due to NC transport. The impurity powder-dropping method is now considered a real-time wall conditioning method for such devices. Based on these results, this method could improve plasma performance and help flush out core impurities.

ACKNOWLEDGMENTS

This work has been carried out within the framework of the EUROfusion Consortium, funded by the European Union via the Euratom Research and Training Programme (Grant Agreement No 101052200 - EUROfusion). Views and opinions expressed are however those of the author(s) only and

do not necessarily reflect those of the European Union or the European Commission. Neither the European Union nor the European Commission can be held responsible for them. It is partially financed by grants PID2020-116599RB-I00 and PID2023-148697OB-I00 funded by MCIN/AEI/ 10.13039/501100011-033 and by ERDF, A Way of Making Europe. It is partially supported also by the U.S. DOE under Contract No. DE-AC02-09CH11466 with Princeton University, by JSPS KAKENHI JP23KK0054 and by NIFS grant administrative budgets (10203010LHD105 and 10201010PSU003). Computing resources were provided on the computer Stellar operated by the Princeton Plasma Physics Laboratory and Princeton Institute for Computational Science and Engineering.

- [1] H. Maaßberg, C. D. Beidler and E. E. Simmet, *Plasma Phys. Control. Fusion* 41, 1135 (1999).
- [2] S. Sudo, *Plasma Phys. Control. Fusion* 58, 043001 (2016)
- [3] B. Burhenn et al., *Nucl. Fusion* 49, 065005 (2009).
- [4] K. Tanaka et al., *Fusion Sci. Tech.* 58, 70 (2010).
- [5] K. Ida et al., *Phys. Plasmas* 16, 056111 (2009).
- [6] K. Tanaka et al., *Plasma Fusion Res.* 5, S2053 (2010).
- [7] D. R. Mikkelsen et al., *Phys. Plasmas* 21, 082302 (2014).
- [8] M. Nunami et al., *Phys. Plasmas* 27, 052501 (2020).
- [9] N. Tamura et al., *Plasma Phys. Control. Fusion* 58, 114003 (2016).
- [10] N. Tamura et al., *Phys. Plasmas* 24, 056118 (2017).
- [11] S. Sudo and N. Tamura, *Rev. Sci. Instrum.* 83, 023503 (2012).
- [12] F. Nespoli et al., *Nat. Phys.* 18, 350 (2022).
- [13] R. Lunsford et al., *Nucl. Fusion* 62, 086021 (2022).
- [14] F. Nespoli et al., *Nucl. Fusion* 63, 076001 (2023).
- [15] A. Iiyoshi et al., *Fusion Tech.* 17, 169 (1990).
- [16] K. Kawahata et al., *Fusion Sci. Tech.* 58, 331 (2010).
- [17] M. Yoshinuma et al., *Fusion Sci. Tech.* 58, 375 (2017).
- [18] K. Tanaka et al., *Rev. Sci. Instrum.* 79, 10E702 (2008)
- [19] Y. Kawamoto et al., *Plasma Fusion Res.* 16, 2402072 (2021).
- [20] M. Goto et al., *Fusion Sci. Tech.* 58, 394 (2010).
- [21] A. Nagy et al., *Rev. Sci. Instrum.* 89, 10K121 (2018).
- [22] N. Tamura et al., *Rev. Sci. Instrum.* 87, 11D619 (2016).
- [23] R. Bussiahn et al., *Plasma Phys. Control. Fusion* 66, 115020 (2024).
- [24] J. Miyazawa et al., *J. Nucl. Mat.* 313-316, 534 (2003).
- [25] J.L. Schwob et al., *Rev. Sci. Instrum.* 58, 1601 (1987).
- [26] K. Berhinger, *JET Report*, JET-R (87) 08 (1987).
- [27] P. Goncharov et al., *Plasma Fusion Res.* 2, 51132 (2007).
- [28] T. Kinoshita et al., *Phys. Rev. Lett.* 132, 235101 (2024).
- [29] K. Tanaka et al., *Nucl. Fusion* 57, 116005 (2017).
- [30] M. Landreman, H. M. Smith, A. Mollén, and P. Helander, *Phys. Plasmas* 21, 042503 (2014).
- [31] S. Buller et al., *J. Plasma Phys.* 85, 175850401 (2019).
- [32] T. Klinger et al., *Nucl. Fusion* 59, 112004 (2019).